

BSPE 00508-880

레디오존데를 이용한 남극
세종기지에서서의 특별고층기상관측

A Preliminary Meteorological Observation
of the Upper Atmosphere using a
Radiosonde System at King Sejong Station,
Antarctica

1995. 3.

한국해양연구소

제 출 문

한국해양연구소 소장 귀하

본 보고서를 “레디오존데를 이용한 남극 세종기지에서의
특별 고층기상관측” 사업의 최종 보고서로 제출합니다.

1995년 3월

한국해양연구소

연구책임자: 원영인, 김예동

참여연구원: 이방용

박순용

김철희

요 약 문

I. 제 목

레디오존데를 이용한 남극 세종기지에서의 특별고층기상관측

II. 연구개발의 목적 및 중요성

날로 심화되어 가는 환경문제를 이해하기 위하여 인간의 활동이 거의 없는 지역에서의 대기상태를 이해하는 것이 필수적이다. 이러한 목적하에 금번 특별기상관측에서는 남극 세종기지에서의 대기층의 구조적 특징을 파악하고자 한다. 대기층의 구조적 특징은 인간의 활동으로 인하여 생성된 오염물질이 어떻게 원격지역까지 영향을 미칠수 있는지를 이해하는데 필수적이다.

본 연구에서는 고층기상관측에 가장 많이 쓰이고 있는 레이더 존데 시스템을 이용, 세종기지 상공의 대기연직구조를 시험적으로 관측하려 한다. 이번 예비관측은 향후 본격적으로 추진될 남극 고층대기연구에 대비하여 극지방에서의 장비운영에 관련된 제반사항에 대해 사전준비작업의 일환으로 수행하며, 또한 이렇게 얻어진 자료가 극지방에서의 오염물질의 이동되는 과정을

이해하는데 어떠한 역할을 하는지 알아본다. 아울러, 이번연구를 통해 그 파괴현상이 두드러진 남극 성층권의 오존층에 대해, 향후 본격적인 연구를 위한 기초연구로서 기구를 이용한 오존관측에 따른 제반 기술적 문제점을 사전 검토하려고 한다.

III. 연구 내용 및 범위

- 남극 세종과학 기지에서 시한적으로 대기의 연직구조를 관측
- 지상기상관측자료(기온, 기압, 바람, 일사량등)의 수집
- 관측자료로부터 대기일변화 양상파악
- 향후 오존관측에 따른 기술적 문제점 검토

IV. 연구결과 및 제언

본 연구에서는 고층기상관측에 가장 많이 쓰이고 있는 레이더 존데 시스템을 이용, 세종기지 상공의 대기연직구조를 시험적으로 관측하였다. 이번 예비관측은 향후 본격적으로 추진될 남극 오존연구에 대비하여 극지방에서의 장비운영에 관련된 제반사항에 대해 사전준비작업의 일환으로 수행되었다. 자료는 약 30 km 까지 얻을 수 있었으며 관측자료로부터 도출된 결과는

대략 다음과 같다. 약 8 km 부근에서 항상 제트기류가 관측되었고 이 제트기류는 서풍일 때 속도가 가장 높게 나타났다. 또한 풍향이 북풍계열로 바뀌면서 제트기류의 속도가 감소된 것을 관측할 수 있었다. 이때는 약 5km 부근에 약한 제트성 기류가 아울러 관측되었으며 이는 상층 제트기류로부터 운동량 (momentum)이 전달되어진 결과로 추정된다.

SUMMARY

I. Title

A Preliminary Meteorological Observation of the Upper Atmosphere using a Radiosonde System at King Sejong Station, Antarctica

II. Abstract

The balloon-borne measurement of the vertical structure of the atmosphere was performed at King Sejong Station (Geographic: 62.6° S, 301.3° E) as a preliminary experiment for the up-coming stratospheric ozone study. Among the common features is the occurrence of jet stream at ~8 km where the tropopause is located. The observed maximum wind speed is larger when the direction of the wind is at about 270 degrees and is stationary between 5 to 15 km height levels. The maximum wind, on the other hand, is lower when the wind blows from the north and when there is a rapid change in the wind direction at above and below the tropopause height. Jet-like winds were also observed at ~5 km height when the maximum wind speed is severely reduced and the occurrence of jet-like winds can be attributed to the downward momentum transportation from the jet streams above.

목 차

요 약 문	3
그림 목차	9
1. 서 론	11
2. 연구 장비	12
3. 결과 및 토의	14
4. 참고문헌	18

CONTENTS

Summary	6
List of Figures	9
1. Introduction	11
2. Instrument	12
3. Results and Discussion	14
4. References	18

List of Figures

Figure 1. The AIR Radiotheodolite with its components illustrated.	19
Figure 2. The radiosonde measures temperature, humidity, and pressure with digital precision. Sensor output is converted to digital words in the radiosonde and, then, transmitted to the ground station.	20
Figure 3. Vertical profiles of air temperature, relative humidity, wind speed, and wind direction at King Sejong Station at 23 LST of Dec. 21, 1994.	21
Figure 3. Vertical profiles of air temperature, relative humidity, wind speed, and wind direction at King Sejong Station at 23 LST of Dec. 21, 1994.	21
Figure 4. Same as Figure 3, but at 21 LST, Dec. 22, 1994.	22
Figure 5. Same as Figure 3, but at 24 LST, Dec. 22, 1994.	23
Figure 6. Same as Figure 3, but at 03 LST, Dec. 23, 1994.	24
Figure 7. Same as Figure 3, but at 06 LST, Dec. 23, 1994.	25
Figure 8. Same as Figure 3, but at 09 LST, Dec. 23, 1994.	26
Figure 9. Same as Figure 3, but at 12 LST, Dec. 23, 1994.	27
Figure 10. Same as Figure 3, but at 15 LST, Dec. 23, 1994.	28

Figure 11. Same as Figure 3, but at 18 LST, Dec.
23, 1994. 29

Figure 12. Same as Figure 3, but at 21 LST, Dec.
23, 1994. 30

1. Introduction

It is essential to detect changes in the Earth system that are occurring now. The Antarctic environment offers a number of unique opportunities for doing this because of favorable observing conditions which include remoteness from anthropogenic emission to the atmosphere and ocean, and potential amplification of climate change at high latitude. A particular important Antarctic atmospheric process is the depletion of ozone as a consequence of the impact of man-made chemicals and changes of stratospheric circulation patterns, producing the so-called Antarctic ozone hole. The link between halocarbons and seasonal ozone variations, through complex photochemistry in the polar night and with the return of the Sun, is established but is not yet fully understood. In order to enhance our knowledge of the detailed mechanism related to the variation of stratospheric ozone concentration, studies of dynamical processes must be addressed as well as studies of the chemical processes, which are known to play an important role in the stratospheric ozone concentration.

A new scientific program of monitoring stratospheric ozone concentration and ultraviolet radiation fluxes is being considered for beginning in near future and, as a preliminary step, we have conducted balloon-borne measurements of the vertical structure of lower atmosphere at King Sejong Station, on the King George Island, Antarctica. We have launched total 10 radiosondes to investigate the structure of the lower

atmosphere during our deployment on the 8th Antarctic Research Program period (December 1994 - January 1995). This experiment was performed for the first time at King Sejong station and here we report some preliminary results from this radiosounding program.

2. Instrument

For this study, a system from Atmospheric Instrumentation Research, Inc. (AIR, Inc.) has been used. A radiosonde is a balloon-borne instrument for the measurement of pressure, temperature, humidity, and wind speed and direction through it passes. It is a complete, fully automatic, all weather, upper-air sounding station that processes radiosonde data in real time. The instrument consists of *an automatic radio theodolite, personal computer-based ground processing system, and a microprocessor-controlled digital radiosonde.*

The AIR Radiotheodolite (Figure 1) consists of a flat phased array antenna with the microprocessor-controller circuit board and a 1680 MHz receiver mounted in compartments in the back panel; a pedestal assembly with azimuth and elevation drives, power supply, and RS-232 data I/O port; and collapsing tripod with leveling mechanism. All tracking and positioning is achieved via direct digital control with control algorithms stored in ROM computer memory. The receiver is mounted in the back of the antenna frame.

The radiosonde signal transmission is processed by the receiver and output to the ground station.

The ground station consists of an IBM PC-compatible personal computer with AIR, Inc. MET-Decoder circuit card, and serial/parallel interface adapters. The ground station PC is used for hardware control, data acquisition and processing, and system communications. Data is stored on the hard disk or on high density 3.5- or 5.25-inch flexible disks for later use.

The Radiosonde (Figure 2) is controlled by an 8-bit microprocessor. Measured values of pressure, temperature and relative humidity (PTU) are telemetered with high-reliability Manchester digital encoding at 1680 MHz every one-two seconds. Temperature is measured by a precision thermistor which is protected by a reflective coating to minimize radiation errors at high altitude. The small mass of the sensor yields fast temperature response. Relative humidity is measured by a carbon hygistor which is mounted in a double shielded aerodynamic duct. The duct is an integral part of the radiosonde housing and shields the hygistor from rain and thermal radiation while exposing it to the flow of ambient air. An AIR, Inc. patented capacitance type pressure sensor is incorporated into these sondes providing precise pressure-altitude determination. An internal temperature sensor located near the pressure sensor provides accurate, automatic temperature compensation. Wind speed and wind direction are determined using radio direction finding combined with the radiosonde height computed from integration of the hydrostatic equation.

3. Results and Discussion

The balloon-borne measurements were carried out at King Sejong Station, King George Island. Balloons of 300 grams and 600 grams in weight were used for launching radiosondes. Each balloon was inflated as to give an ascension rate of ~ 7 m/s. Figure 3 shows an example of temperature and wind profile measured at 23 LST, Dec. 21, 1994. The most obvious feature from the sounding is the presence of jet stream near the 9 km level where the tropopause is located. The temperature decreases with altitude below the tropopause with a lapse rate of ~ 5.6 °C and then reverse to increase with height above the tropopause. The sharp increase of relative humidity near at 2 km and 4 km height indicates the presence of cloud layers at these levels.

Usually, the surface wind blew so strong that it was hard to inflate and float the balloon. In regard to this, we chose the time of observation when the surface condition was relatively favorable for the release of the sonde. The surface wind became moderate in the evening of Dec. 22, 1994 and we started continuous observations from 21 LST, Dec. 22 through 21 LST, Dec. 23, 1994 at three-hour interval (one full day) for the investigation of the diurnal variation of the atmospheric structure.

Figure 4 through 12 illustrate the wind, temperature, and the relative humidity structures measured during one day period. The data were acquired up to ~ 30 km height in most cases; except for few measurements when either

the system lost the tracking of sondes or the balloon was exploded during the ascent. The temperature profile does not seem to change much throughout the one day period. The surface temperature in this season remained near 0° C and the minimum temperature, ranging from 48 to 54° C below zero, occurred near the tropopause height (~8 km). The distinct jet stream was observed for all measurements during this period with its speed varying considerably. The maximum wind speeds for the first three measurements (Figure 4,5 and 6) of the one day observation were in the range of 30 to 35 m/s. Then at 09 LST Dec. 23 (Figure 8), the jet stream reduced its speed down to 25 m/s and the decrease of the maximum wind speed continued for the rest of observations. Data is not available above 3 km height at 06 LST, Dec. 23 and no specific comment can be inferred from Figure 8. Later at 09 LST Dec. 23, when the maximum wind speed started to decrease, the wind direction near the tropopause height has been shifted southward. At 12 LST, Dec. 23, the wind direction is again near 300 degrees at the tropopause height with a maximum speed of 20 m/s. For observations at 09 LST and 12 LST, Dec. 23, northeasteries are seen above the height of maximum wind speed where the previous three observations revealed no change of wind direction from 5 to 15 km height region. The northeasteries, seen at 09 LST and 12 LST, Dec. 23, above the tropopause is obstructive to the flow of the jet stream and may be related to the observed reduction of jet stream at the tropopause height. Another feature seen from the observations at 09 LST and 12 LST, Dec. 23 is the occurrence of low-level jet-like winds near at ~5 km height. As was pointed out by Choi (1991), the coastal low-level jet-like

wind seen in Figures 8 and 9 may be associated with the upper tropospheric jet stream due to the downward momentum transport. The upper tropospheric jet stream further reduced its speed down to ~ 18 m/s at 15 LST, Dec. 23 as illustrated in Figure 10. The wind at this time blows from the west at surface and gradually changes its direction clockwise up to the tropopause height. This trend is reversed and the direction of the wind rapidly changed counter-clockwise between 10 to 15 km. The results of the last two observations (Figures 11 and 12) show maximum wind speed at less than 15 m/s, which are now too low to be jet streams. On the other hand, the low-level jet-like wind seen from Figures 8 and 9 became more distinct and the height of its location lowered down to ~ 3 km. Another distinct wind peaks are also seen at the altitude of ~ 17 km for the last two measurements. The momentum lost at the tropopause height seemed to have been transported to up- and downward since the observed secondary wind peaks at above and below the tropopause are more clear when the maximum wind speed is reduced considerably.

We have examined the variation of upper atmospheric structure up to 30 km observed from 21 LST, Dec. 22 through 21 LST, Dec. 23, 1994. The temperature profile does not change much during the time of observations. A lapse rate of $\sim 5.6^\circ$ is observed up to the tropopause height (~ 8 km) and a moderate increase of temperature is seen above the 10 km height at a rate of $\sim 0.9^\circ/\text{km}$. The wind speed increases with height from the surface and reaches its maximum at about 8 km. The reversed trend continues with height above the tropopause and then increases again above at ~ 20 km. No general wind pattern is seen below the tropopause height but a characteristic tendency from

all measurements is that the wind direction changes in a counter-clockwise direction above 20 km. The jet stream at the altitude of ~8 km is a common feature from all measurement; however its speed changes with a considerable fluctuation. The maximum wind speed is larger when the wind direction is at about 270 degrees (westerlies) and is stationary between 5 to 15 km height. On the other hand, the upper tropospheric jet stream becomes weak when the wind blows from the north and when there is a rapid changes in the wind direction at above and below the tropopause height. When the maximum wind speed was reduced, jet-like winds appeared near the 5 km height and the location of those got lowered when the maximum wind speed decreased significantly.

References

- Ball, F.K., The theory of strong katabatic winds, *Aust. J. Physics.*, Vol. 9, 373-386, 1956.
- Choi, Hyo, Structure of jet-like winds in the lower atmosphere, King George Island, Antarctica, *Korea Journal of Polar Research*, Vol. 2, 197-202, 1991.
- Kawaguchi, Sadao, S. Kobayashi, N. Ishikawa, and T. Ohata, Aerological soundings of the surface boundary layer at Mizuho Station, East Antarctica, *Proceed. of the Fourth Symposium on Polar Meteorology and Glaciology, Special Issue, No. 24*, 77-86, 1982.
- Mather, K.B., and G.S. Miller, Notes on topographic factors affecting the surface wind in Antarctica, with special reference to katabatic winds, *Univ. Alaska, Tech. Rep., UAG-R-189*, 125, 1967
- Matsuhara, T. Ueno, T. Sakamoto, K. Matsuhara, and S. Kawaguchi, Some characteristics of wind and temperature changes in the Syowa Area, Antarctica, in terms of katabatic wind, *Proceed. of the Fourth Symposium on Polar Meteorology and Glaciology, Special Issue, No. 24*, 87-93, 1982.

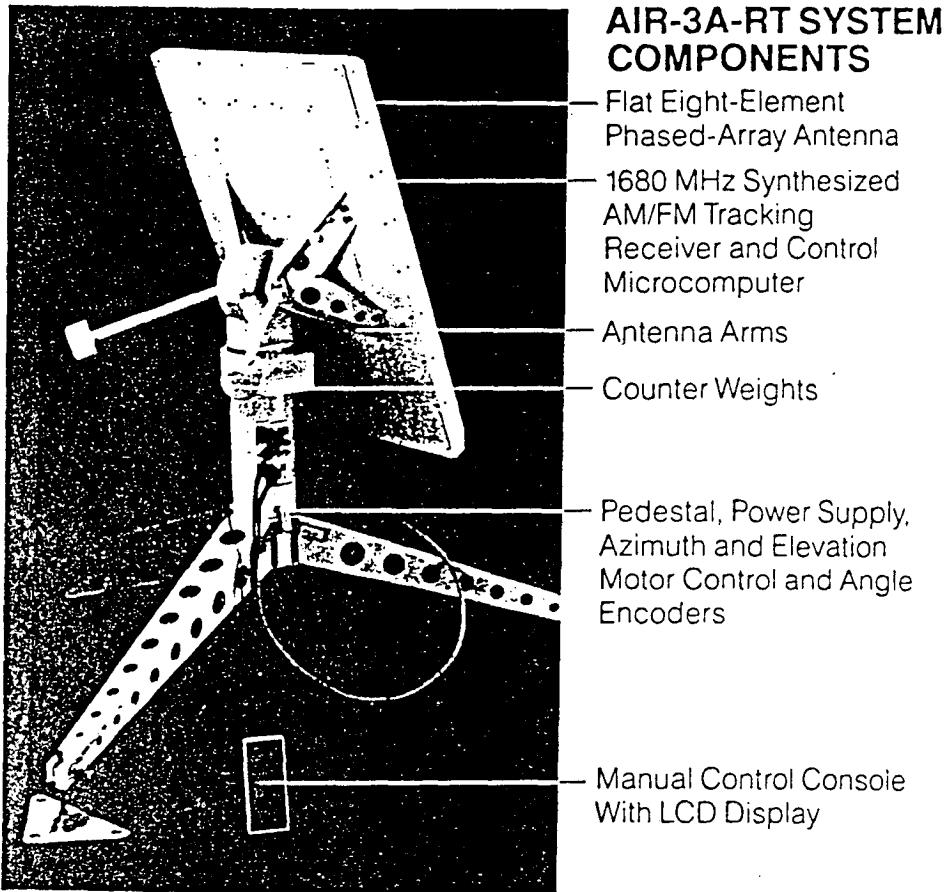


Figure 1. The AIR Radiotheodolite with its components illustrated.

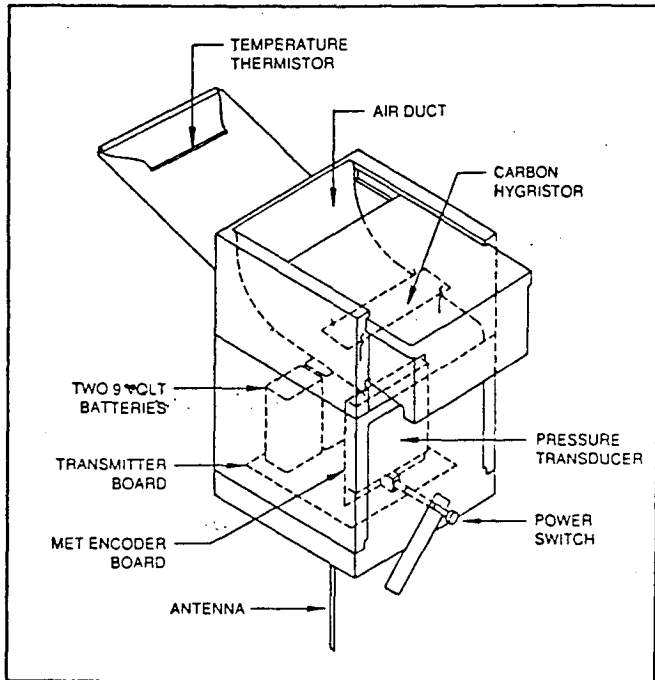


Figure 2. The radiosonde measures temperature, humidity, and pressure with digital precision. Sensor output is converted to digital words in the radiosonde and, then, transmitted to the ground station.

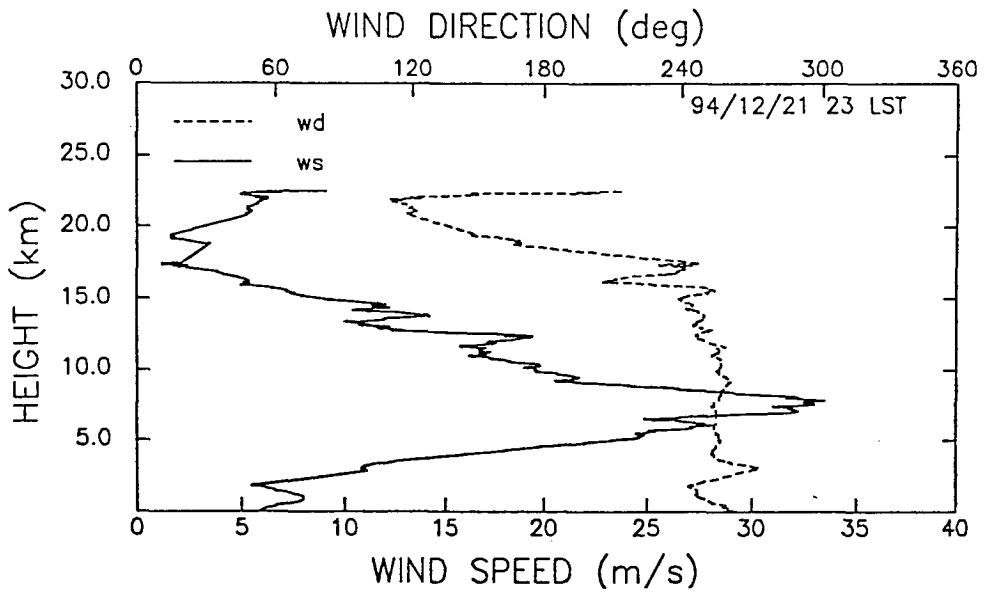
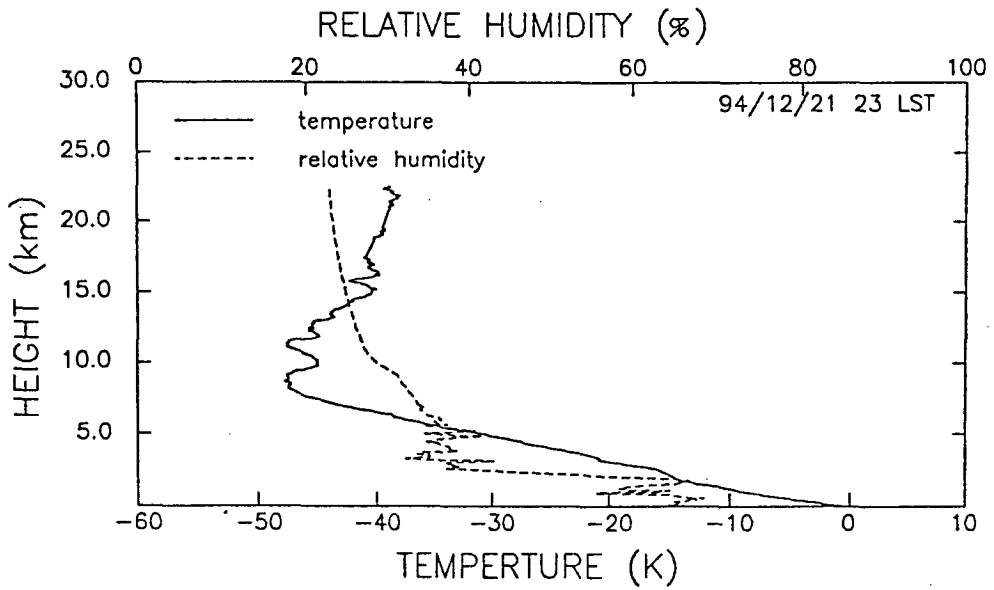


Figure 3. Vertical profiles of air temperature, relative humidity, wind speed, and wind direction at King Sejong Station at 21 LST of December 21, 1994.

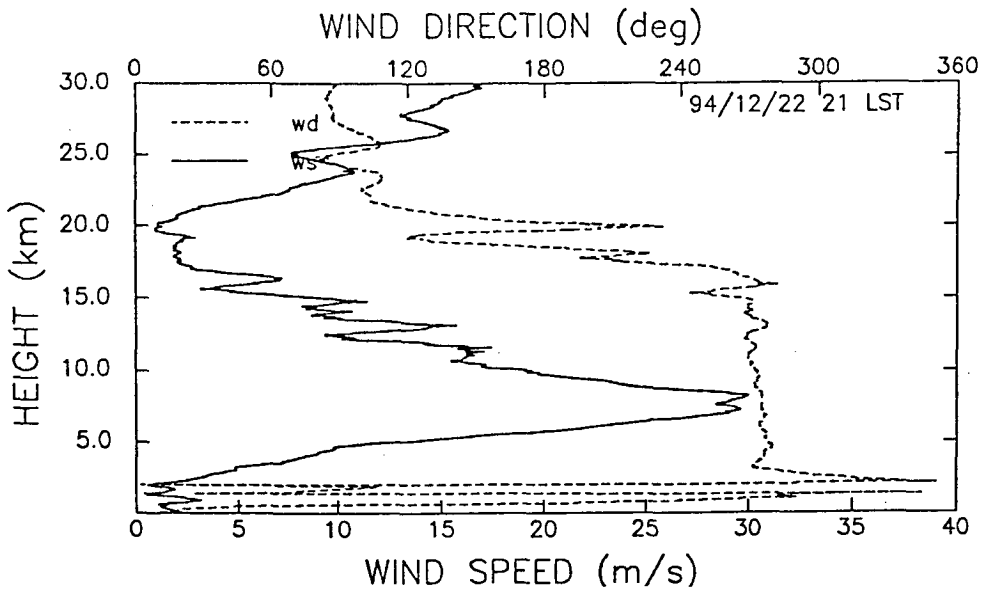
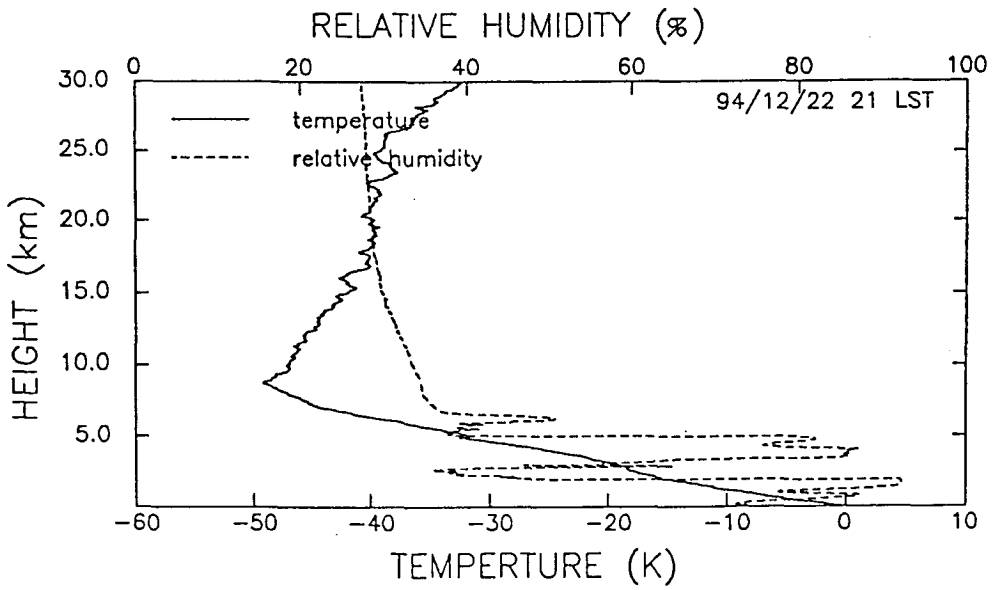


Figure 4. Same as Figure 3, but at 21 LST, December 22, 1994

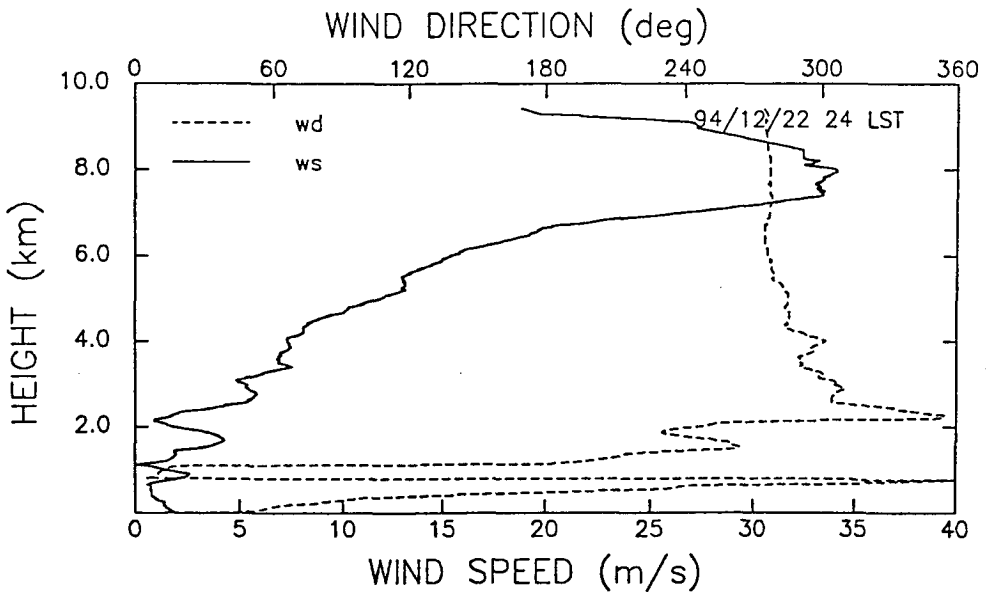
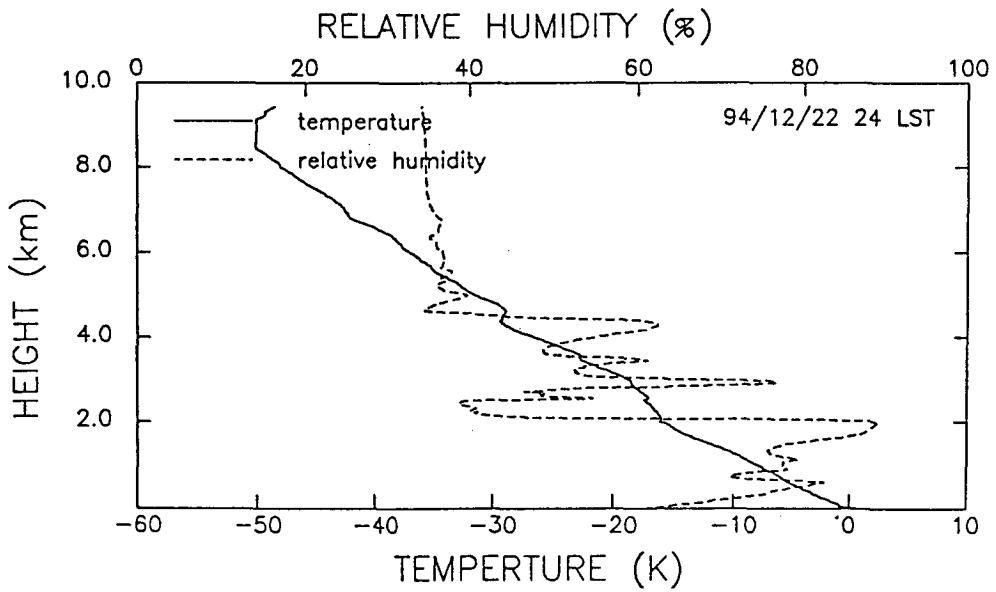


Figure 5. Same as Figure 3, but at 24 LST, December 22, 1994

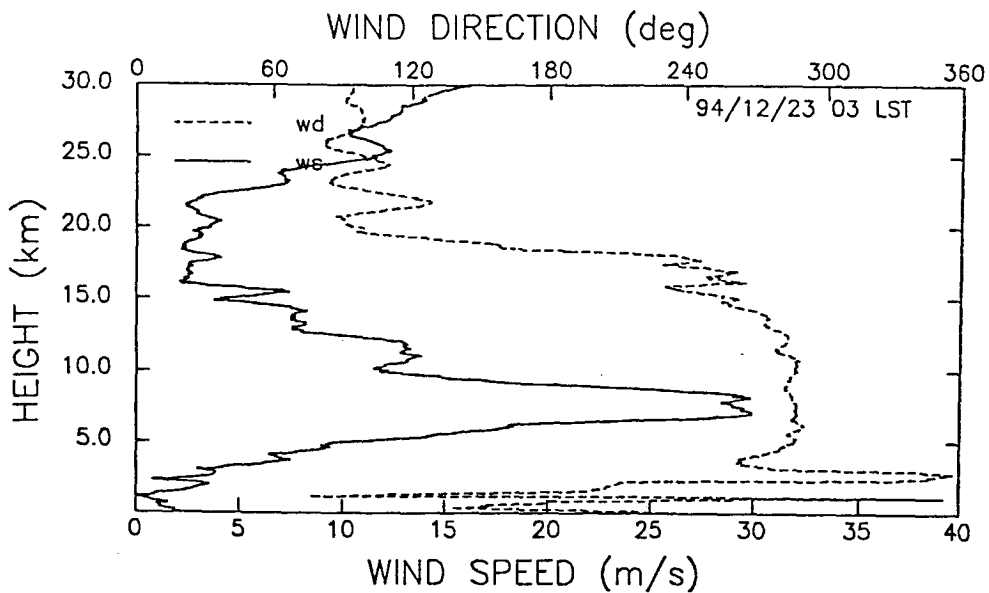
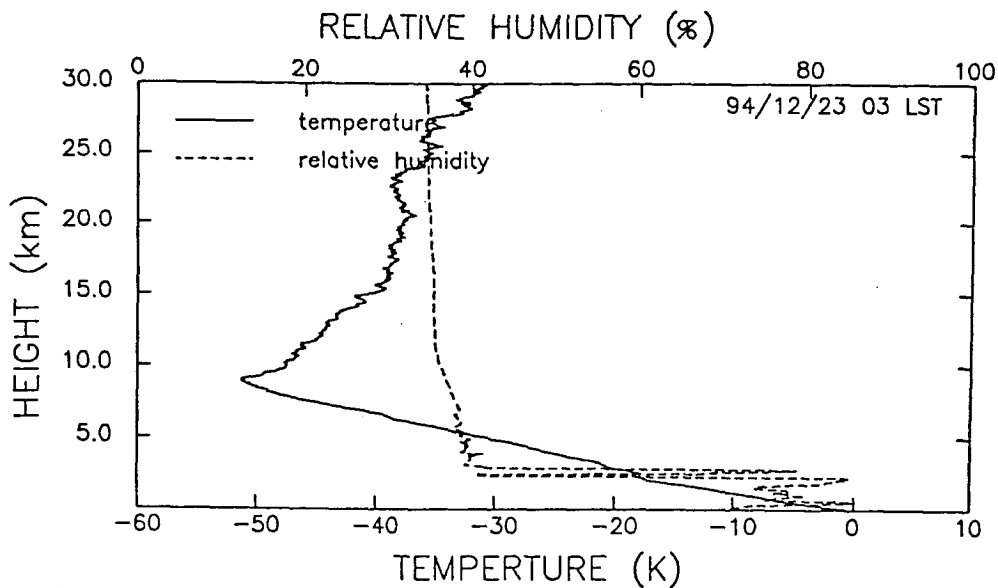


Figure 6. Same as Figure 3, but at 03 LST, December 23, 1994

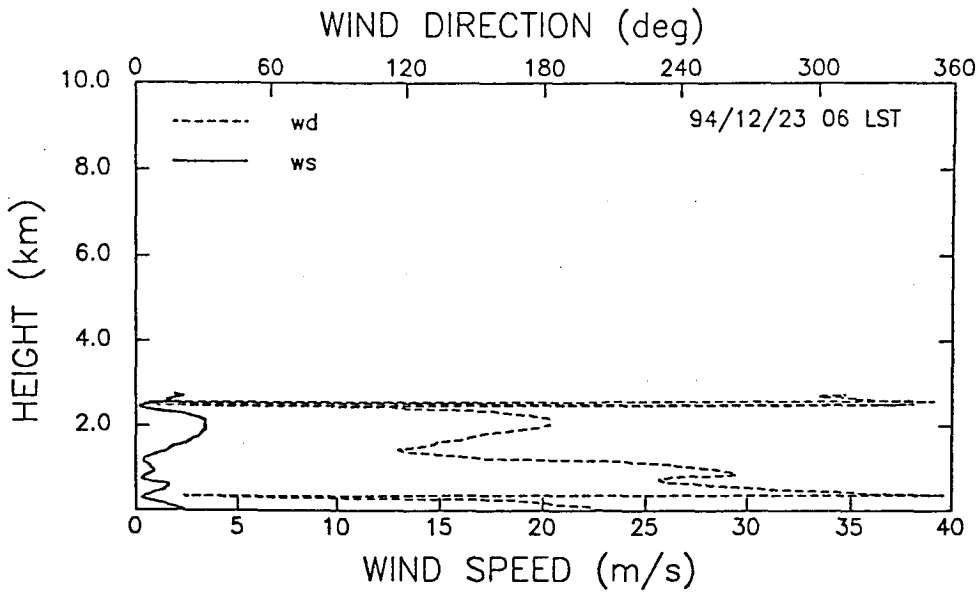
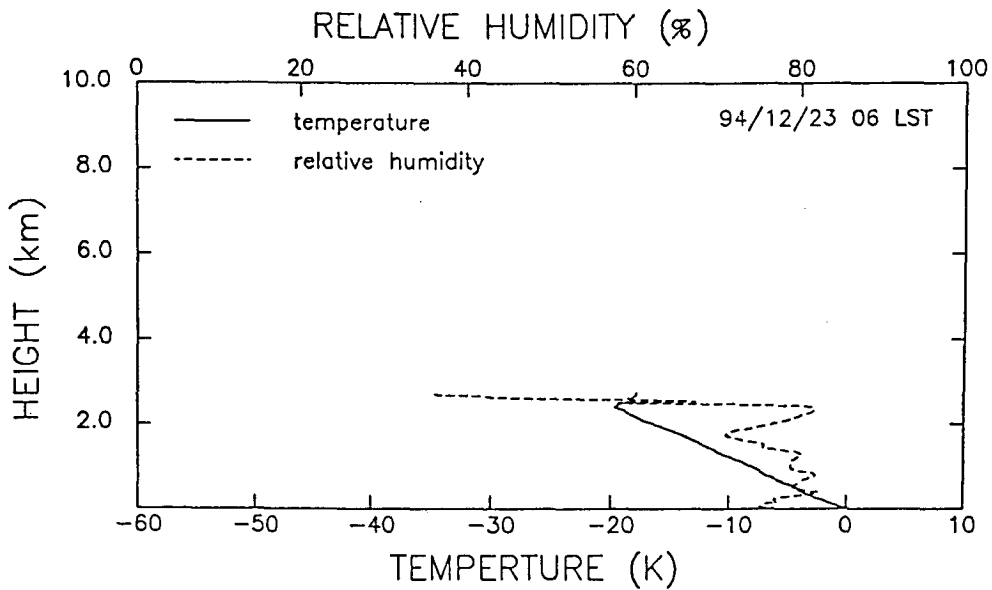


Figure 7. Same as Figure 3, but at 06 LST, December 23, 1994

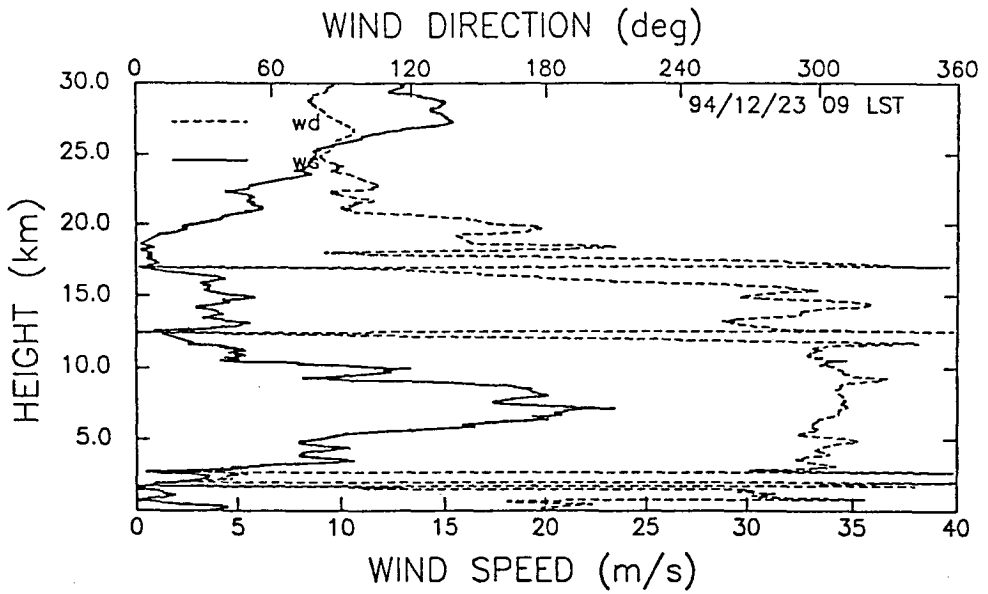
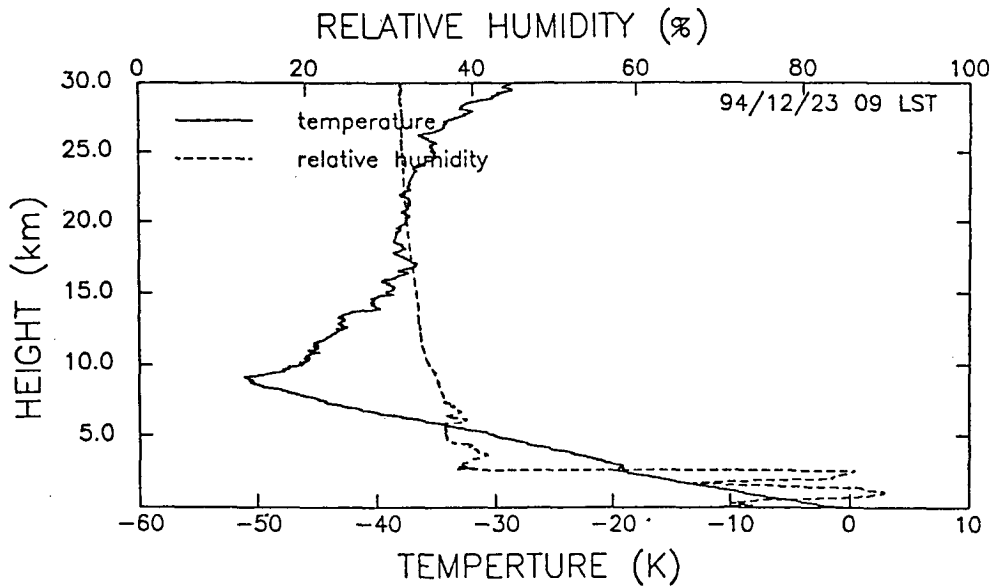


Figure 8. Same as Figure 3, but at 09 LST, December 23, 1994

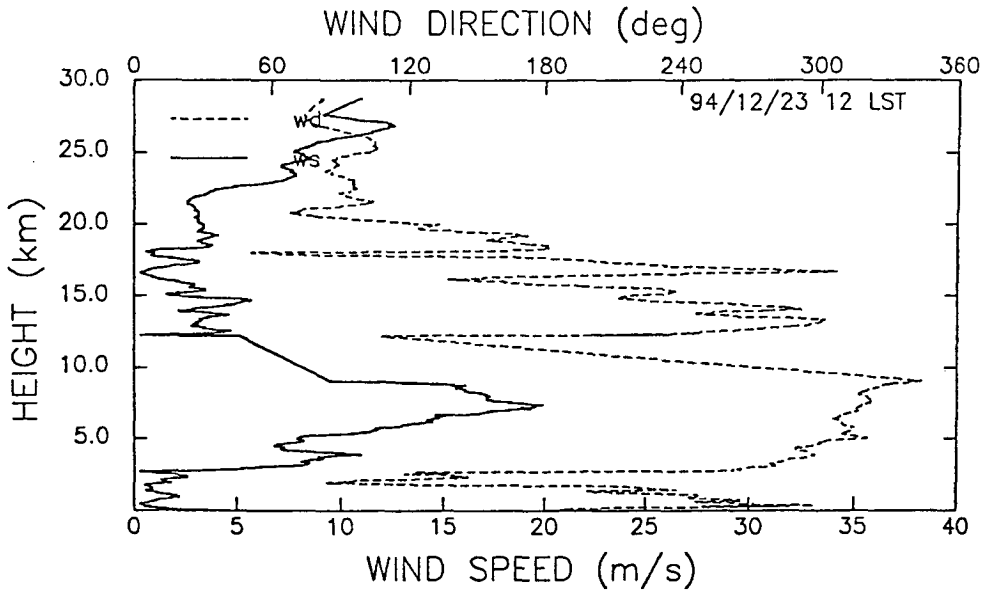
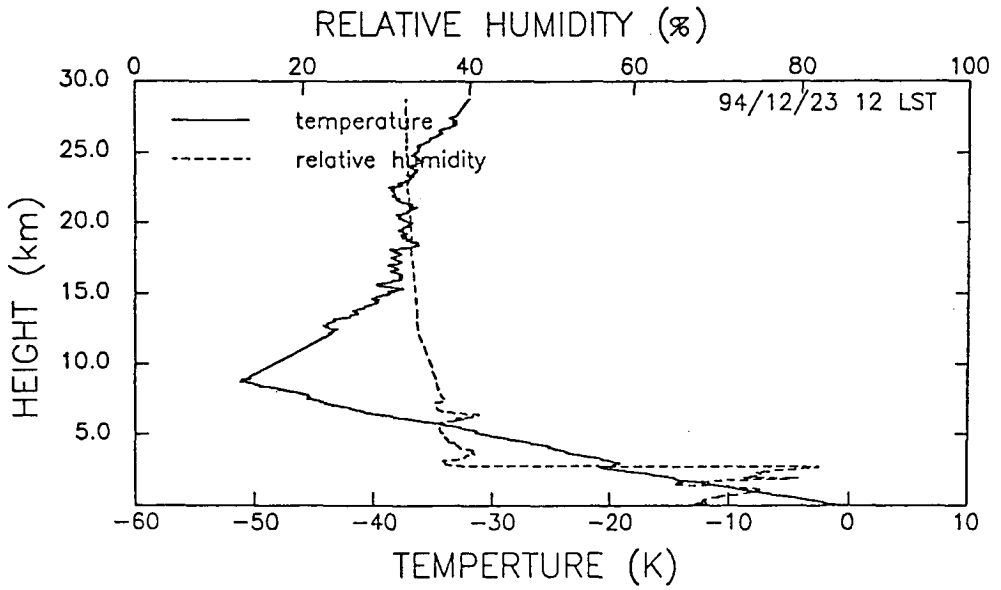


Figure 9. Same as Figure 3, but at 12 LST, December 23, 1994

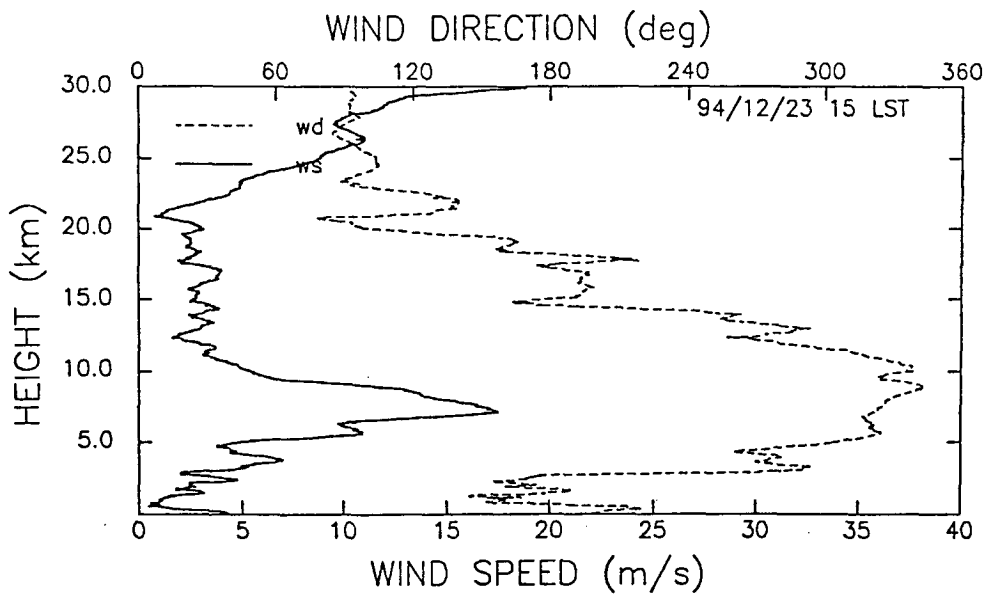
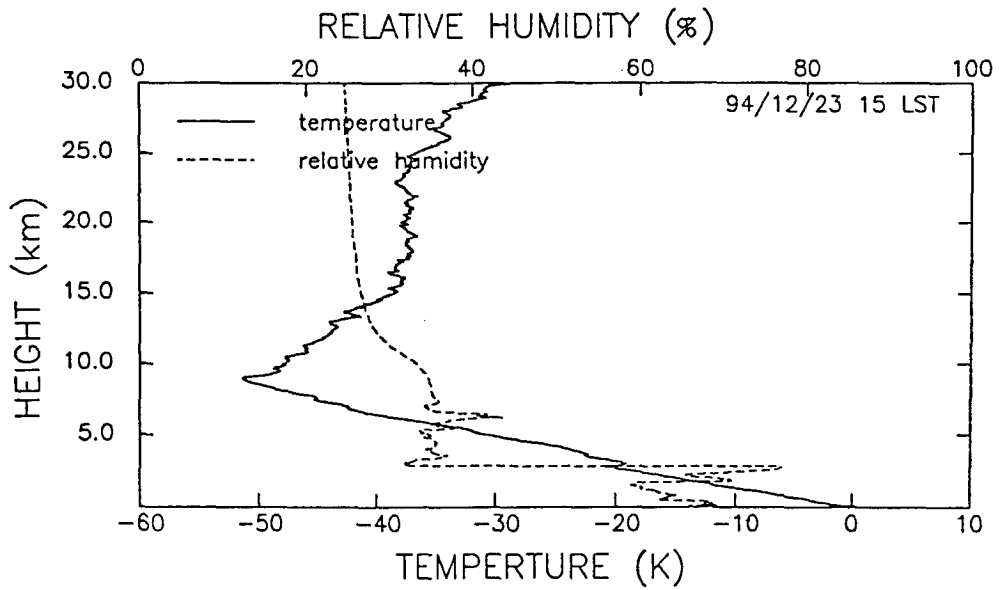


Figure 10. Same as Figure 3, but at 15 LST, December 23, 1994

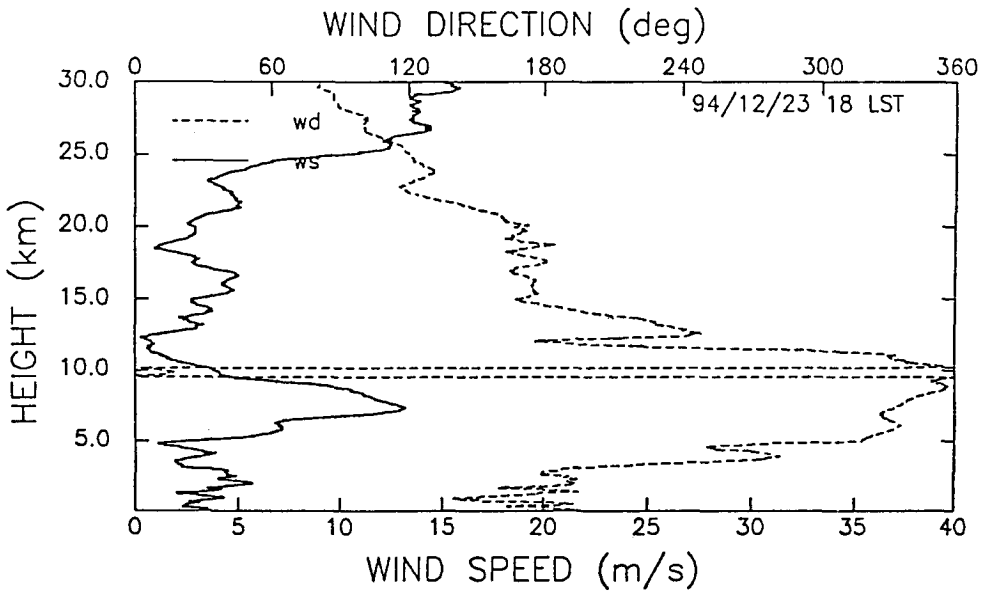
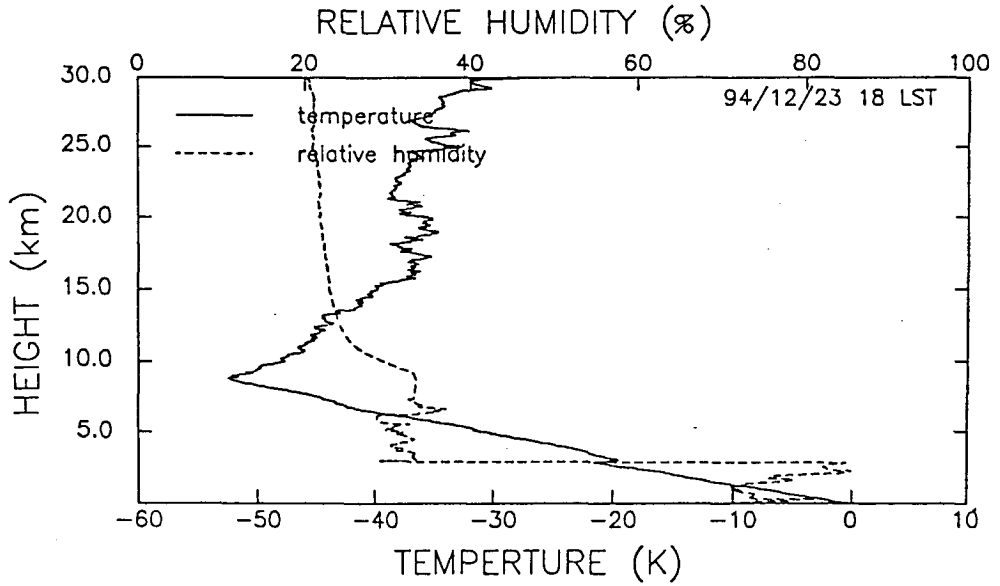


Figure 11. Same as Figure 3, but at 18 LST, December 23, 1994

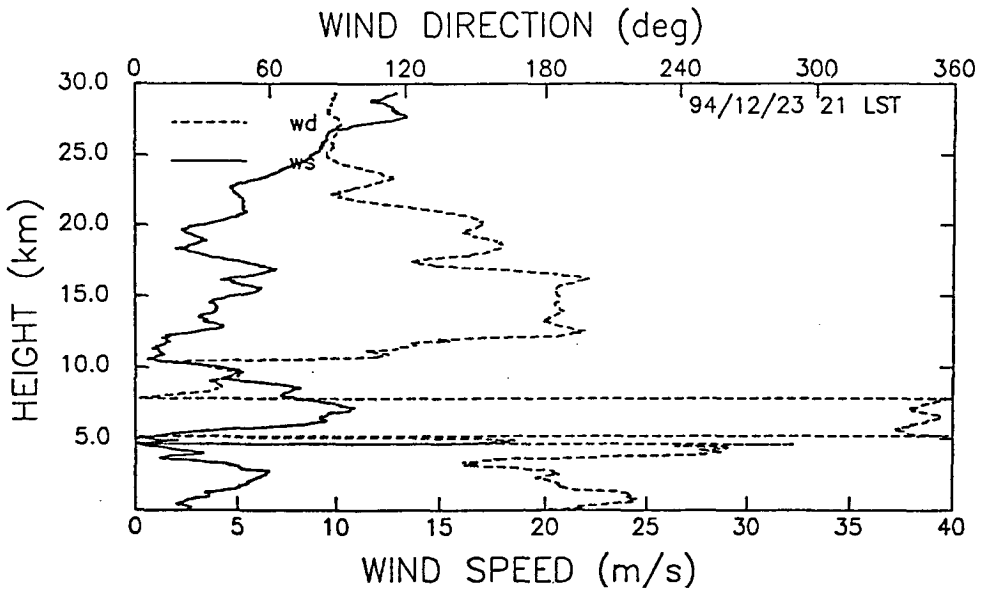
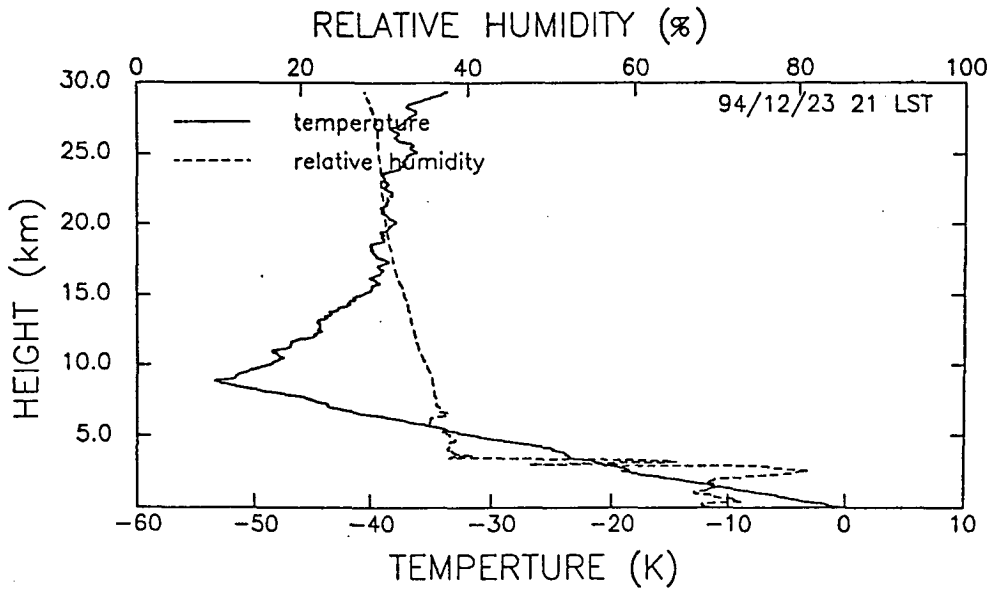


Figure 12. Same as Figure 3, but at 21 LST, December 23, 1994